



**IDEA**

---

**Innovations Deserving  
Exploratory Analysis Programs**

***Rail Safety IDEA Program***

---

## **RAILROAD BRIDGE DYNAMICS AND RATINGS**

Final Report for Rail Safety IDEA Project 24

Prepared by:  
Kevin Bollinger,  
Hatch Mott MacDonald  
Chicago, IL

***June 2015***

---

**TRANSPORTATION RESEARCH BOARD**  
*OF THE NATIONAL ACADEMIES*

## **Innovations Deserving Exploratory Analysis (IDEA) Programs Managed by the Transportation Research Board**

- This IDEA project was funded by the Safety IDEA Program.

The TRB currently manages the following three IDEA programs:

- NCHRP IDEA Program, which focuses on advances in the design, construction, and maintenance of highway systems, is funded by American Association of State Highway and Transportation Officials (AASHTO) as part of the National Cooperative Highway Research Program (NCHRP).
  - Safety IDEA Program, which focuses on innovative approaches for improving railroad safety and performance. The Safety IDEA program is funded by the Federal Railroad Administration (FRA).
  - The Transit IDEA Program, which supports development and testing of innovative concepts and methods for advancing transit practice, is funded by the Federal Transit Administration (FTA) as part of the Transit Cooperative Research Program (TCRP).
- Management of the three IDEA programs is coordinated to promote the development and testing of innovative concepts, methods, and technologies.
  - For information on the IDEA programs, check the IDEA website ([www.trb.org/idea](http://www.trb.org/idea)). For questions, contact the IDEA programs office by telephone at (202) 334-3310.

- IDEA Programs  
Transportation Research Board  
500 Fifth Street, NW  
Washington, DC 20001

- The project that is the subject of this contractor-authored report was a part of the Innovations Deserving Exploratory Analysis (IDEA) Programs, which are managed by the Transportation Research Board (TRB) with the approval of the Governing Board of the National Research Council. The members of the oversight committee that monitored the project and reviewed the report were chosen for their special competencies and with regard for appropriate balance. The views expressed in this report are those of the contractor who conducted the investigation documented in this report and do not necessarily reflect those of the Transportation Research Board, the National Research Council, or the sponsors of the IDEA Programs. This document has not been edited by TRB.
- The Transportation Research Board of the National Academies, the National Research Council, and the organizations that sponsor the IDEA Programs do not endorse products or manufacturers. Trade or manufacturers' names appear herein solely because they are considered essential to the object of the investigation.

*Railroad Bridge Dynamics and Ratings*

IDEA Program Final Report

For the Period May 2013 through November 2014

Contract Number: Safety-24

**Prepared for the IDEA Program  
Transportation Research Board  
National Research Council**

Kevin Bollinger



120 S. LaSalle Street, Suite 1240  
Chicago, IL 60603

**June 2015**

## **Acknowledgments**

This research was supported by the National Academies' Transportation Research Board (TRB) IDEA Program. The project, "High-Speed Rail Bridge Dynamics and Ratings," is part of the Safety IDEA Program, which is funded by the Federal Railroad Administration. Charles Taylor was the TRB Project Manager.

The author would like to acknowledge the guidance and support provided by the members of the project's Expert Review Panel:

Craig Rolwood, PE, Project Director, Structure Design, Amtrak  
Duane Otter, Ph.D., PE, Transportation Technology Center Inc.  
David Place, P.Eng, Project Director—Crossrail, Mott MacDonald

The author would also like to acknowledge the support of Jim Richter Deputy Chief Engineer, Structures of Amtrak and Amtrak personnel for their active participation in the project, timely answers to questions, access to equipment, and right of entry to property for field testing.

## **Rail Safety IDEA PROGRAM COMMITTEE**

### **CHAIR**

CONRAD RUPPERT JR.  
*University of Illinois*

### **MEMBERS**

MICHAEL FRANKE  
*Amtrak*

PETER FRENCH  
*Association of American Railroads*

BRAD KERCHOF  
*Norfolk Southern Railway*

HENRY LEES JR.  
*BNSF Railway*

STEPHEN POPKIN  
*Research and Innovative Technology Administration*

### **FRA LIAISON**

TAREK OMAR  
*Federal Railroad Administration*

### **NTSB LIAISON**

STEPHEN KLEJST  
*National Transportation Safety Board*

### **TRB LIAISON**

SCOTT BABCOCK  
*Transportation Research Board*

### **TRB TCRP Staff**

STEPHAN A. PARKER, *Senior Program Officer Transit  
Cooperative Research Program*

### **IDEA PROGRAMS STAFF**

STEPHEN R. GODWIN, *Director for Studies and Special  
Programs*

JON M. WILLIAMS, *Program Director, IDEA and Synthesis  
Studies*

JO ALLEN GAUSE, *Senior Program Officer*

CHUCK TAYLOR, *Senior Program Officer*

DEMISHA WILLIAMS, *Senior Program Assistant*

### **EXPERT REVIEW PANEL**

CRAIG ROLWOOD, *Amtrak*

DUANE OTTER, *Transportation Technology Center Inc.*

DAVID PLACE, *Crossrail, Mott MacDonald*

TABLE OF CONTENTS

1 EXECUTIVE SUMMARY .....1

2 MATERIALS REVIEWED.....2

3 NORMAL RATING CALCULATION .....3

3.1 AMTRAK BRIDGE 155.85 OVER THE USQUEPAUG RIVER IN RHODE ISLAND .....3

3.2 NORMAL RATING CALCULATIONS .....4

4 DETERMINATION OF DYNAMIC VERTICAL EFFECTS .....4

4.1 MODELING.....5

4.2 DYNAMIC EQUATIONS AND CALCULATION SOFTWARE.....5

4.2.1 The Moving Load Model .....5

4.2.2 Natural Frequency and Damping Equations .....7

4.2.3 Moving Load Model with Vehicle-Bridge Interaction Considerations.....8

4.2.4 Wheel Load Case.....8

4.3 MODEL AND FIELD RESULTS .....10

4.3.1 Model Verification.....10

4.3.2 Work Train Model Information.....10

4.3.3 Acela Train Model Information .....12

4.3.4 Byers Report.....13

4.4 RESONANT SPEEDS .....15

4.5 CANCELLATION.....15

4.6 DYNAMIC VERTICAL EFFECT (DVE).....15

5 FIELD TESTING .....16

5.1 OVERVIEW.....16

5.2 BRIDGE DESCRIPTION .....16

5.3 INSTRUMENTATION DESCRIPTION.....17

5.4 MONITORING PROCEDURE.....17

5.4.1 TRAINS MONITORED .....18

5.4.2 MONITORING RESULTS .....19

6 PROPOSED RATING PROCEDURE .....23

6.1 NORMAL RATINGS CONSIDERING DYNAMIC CHARACTERISTICS .....23

7 BRIDGE LENGTH AND TRAIN SPEED COMPARISONS .....24

7.1 COMPARISON OF BRIDGE LENGTHS .....24

8 CONCLUSIONS AND RECOMMENDATIONS.....26

9 FUTURE RESEARCH AND CRITERIA DEVELOPMENT .....26

10 REFERENCES .....27

---

## LIST OF TABLES

TABLE 4.1	COMPARISONS OF IMPACT VALUES BETWEEN THE BYERS REPORT AND MATHEMATICAL MODELING
TABLE 6.1	NORMAL BRIDGE RATINGS FOR BR.155.85

## LIST OF FIGURES

FIGURE 3.1	Span details of elevation, plan, and section views (N.Y. N.H. & H.R.R.).
FIGURE 4.1	Motion of a constant force $f$ along a simply supported beam of span $l$ at velocity $c$ .
FIGURE 4.2	Load configuration.
FIGURE 4.3	Six mph train speed induced girder deflections at midspan.
FIGURE 4.4	Forty-one mph train speed induced girder deflections at midspan.
FIGURE 4.5	One-hundred and twenty mph train speed induced girder deflections at midspan superimposed on the quasi-static 6 mph train.
FIGURE 4.6	One-hundred and twenty mph train speed induced girder bending moments at midspan superimposed on the quasi-static 6 mph train.
FIGURE 4.7	One-hundred and forty-five mph train speed induced girder deflections at midspan superimposed on the quasi-static 6 mph train.
FIGURE 4.8	One-hundred and forty-five mph train speed induced girder bending moments at midspan superimposed on the quasi-static 6 mph train.
FIGURE 4.9	Page 1100 of the Byers report illustrating mean percent impact values.
FIGURE 5.1	Amtrak Bridge 155.85.
FIGURE 5.2	String potentiometer mounted near girder bearing.
FIGURE 5.3A	Midspan deflection of east span girders (Amtrak work train, 6 mph).
FIGURE 5.3B	Midspan strain of east-span girders at lower strain gage location 16.125 in. below section centroid - (Amtrak work train, 6 mph).
FIGURE 5.4A	Midspan deflection of east span girders (Amtrak work train, 41 mph).
FIGURE 5.4B	Midspan strain of east span girders at lower strain gage location 16.125 in. below section centroid (Amtrak work train, 41 mph).
FIGURE 5.5A	Midspan deflection of east span girders (Amtrak Acela train, 120 mph).
FIGURE 5.5B	Midspan strain of east span girders at lower strain gage location 6.125 in. below section centroid (Amtrak Acela train, 120 mph).
FIGURE 5.6A	Midspan deflection of east span girders (Amtrak Acela train, 145 mph).
FIGURE 5.6B	Midspan strain of east span girders at lower strain gage location 16.125 in. below section centroid (Amtrak Acela train, 145 mph).
FIGURE 6.1	Flow chart.
FIGURE 7.1	Dynamic vertical effects for a 15-foot span bridge.
FIGURE 7.2	Dynamic vertical effects for bridge 155.85 (36-foot span).
FIGURE 7.3	Dynamic vertical effects for a 60-foot span bridge.
FIGURE 7.4	Dynamic vertical effects for a 80-foot span bridge.
FIGURE 7.5	Dynamic vertical effects for a 100-foot span bridge.
FIGURE 7.6	Dynamic vertical effects for a 150-foot span bridge.

---

# 1 EXECUTIVE SUMMARY

Bridge rating calculations are performed to determine the safe capacity of existing structures. The American Railway Engineering and Maintenance-of-Way Association (AREMA) *Manual for Railway Engineering (MRE)* is the current recommended practice used by the great majority of railroads in North America. The Foreword to MRE Chapter 15, “Steel Structures,” limits the application of the chapter to freight train speeds of up to 70 mph, and passenger train speeds of up to 90 mph. Therefore, the chapter provisions do not provide a method to calculate a bridge rating for train speeds beyond 90 mph.

As speeds increase, impact values either increase or decrease depending on the dynamic characteristics of the bridge structure and equipment using the track. Currently, Amtrak is operating high-speed passenger trains at speeds of up to 150 mph on the Northeast corridor. The research described in this report investigates impact factors for speeds above 90 mph to be used in capacity ratings of existing bridges. To accomplish this, basic structural dynamic methodologies and current structural engineering codes and procedures are utilized in order to propose an impact evaluation methodology consistent with current North American railroad bridge practice.

The current MRE impact equation includes rocking and vertical effect components. The rocking effect reflects the side-to-side movement of a train as it travels down the track, while the vertical effect component reflects the dynamic load amplification effect caused by the following key factors:

- Bridge Stiffness and Mass
- Structure Natural Frequency
- Damping
- Span Length
- Axle Weight and Spacing
- Train Speed.

These factors were applied to various structural dynamic equations and known procedures common in the high-speed rail community. This allowed development of a moving load model used to determine the impact factor for train speeds greater than 90 mph. Results of the moving load model were then compared with field observations taken in November 2013 at Amtrak Bridge 155.85 and prior impact tests reported by William Byers in 1970. A review of the field data demonstrates that the mathematical model compares well with actual bridge responses as shown by the graphs in Section 4.3.

Once the model was verified with field data, calculations were performed establishing dynamic vertical effects at various train speeds, including those that induce resonance. The dynamic vertical effect value at resonance was then inputted into the AREMA MRE impact equation for a normal bridge rating. A flow chart has been developed that illustrates the steps required for an accurate rating calculation.

In addition, calculations of vertical effects for five additional span lengths were completed. Examination of the phenomenon of resonance associated with different bridge span lengths confirms that resonance has a great influence on the dynamic vertical effect associated with the bridge and, as a consequence, the vertical acceleration of the bridge deck.



## 2 MATERIALS REVIEWED

The conclusions developed in this report relied upon several codes, standards, and technical publications.

J.A.L. Waddell, in his book *Bridge Engineering* (1916), presents a historic overview of the early development of impact equations. By 1911, the engineering profession had recognized that the chief factors influencing impact were:

- Unbalanced locomotive drivers
- Rough and uneven track
- Flat or irregular wheels
- Eccentric wheels
- Rapidity of application of load
- Deflection of beams and stringers.

In addition, Waddell reports that the condition of resonance had already been recognized for some time. He states that Professor S.W. Robinson had observed that the maximum impact on a bridge is dependent on how its normal rate of vibration coincides with the times of the series of impulses from applied loads (at this time, from unbalanced locomotive drivers).

J.F. Unsworth, in *Design of Modern Steel Railroad Bridges* (2010), provides a helpful overview of the current AREMA impact calculation procedure. Unsworth describes both components of the impact equation (rocking effect and vertical effect), and notes that rocking effects are independent of train speed.

The EN 1991-2:2003 titled *Eurocode 1: Actions on structures-Part 2: Traffic Loads on Bridges* (2010) contains information pertaining to impact loads to high-speed trains. Once it has been determined that a dynamic analysis within the code is required for a bridge, some of the considerations from the Eurocode are as follows:

- The dynamic effects of a real train may be represented by a series of moving point forces. Vehicle/structure mass interaction effects do not need to be directly calculated.
- The analysis should take into account variations throughout the length of the train in axle forces and the variations in spacing of individual axles or groups of axles.
- For spans less than 30 m (98 feet) dynamic vehicle/bridge mass interaction effects tend to reduce the peak response at resonance. Account may be taken of these effects by carrying out a dynamic vehicle/structure interactive analysis (*note*: the method used should be agreed to by the relevant authority specified in the National Annex of the Eurocode) or increasing the value of damping assumed for the structure according to approved additional damping  $\Delta\beta$  values.

Expanding upon this information, the moving load model developed in this project reflects structural dynamic calculation methods presented in *Dynamics of Railway Bridges* (Fryba 1996) and *Vehicle–Bridge Interaction Dynamics* (Yang 2004). The series of travelling points across a span reflect concepts presented in “Vibration of simple beams due to trains moving at high speeds” (Yang et al. 1977). The impact values developed by the model were reduced to reflect vehicle–bridge interaction because of the overestimation the moving load model induces for bridge span lengths under 100 feet. These reductions in peak impact values were calculated from EN 1991 – 2:2003 (Eurocode). Finally, the impact values were compared with field data obtained on November 22, 2013, for Bridge 155.85 and from the report “Impact from Railway Loading on Steel Girder Spans” (Byers 1970).

While bridge rating typically focuses on structure capacity, satisfactory structural behavior is also important. For high-speed rail bridges, deck acceleration affects passenger comfort and track and bridge structure deterioration (Zacher).

### 3 NORMAL RATING CALCULATION

AREMA's *Manual for Railway Engineering*, Chapter 15, "Steel Structures, Part 7" (2009), and Amtrak's Engineering Practices titled Bridge Load Rating Policy (2011) establish criteria for rating calculations of existing steel railway bridges. The MRE describes calculations for the normal rating of a bridge, determining the capacity appropriate for day-to-day use of the structure. It also describes calculations for the maximum rating of a bridge, the capacity appropriate for occasional use of the structure (typically rare, heavy loads). Unless otherwise specifically noted, this report will focus on the determination of normal ratings. The same impact factor is used for the calculation of both the normal and maximum structure ratings.

The capacity of the member to be rated will be determined by the Cooper E Live Load applied to the member. The Cooper E Equivalents of 2 HHP-8 Electric Locomotives and a train of six Horizon Fleet Coach Cars are provided in Amtrak's Bridge Load Rating Policy. The calculations take into consideration normal rating live loads plus impact stresses and fatigue rating procedures. Since the historic use of the existing line is not known, fatigue procedures will not be considered in this report. Final stress evaluations are based on applying an impact value as a percentage of the live load to the static load. Section 7.3.1 states "Rating of existing bridges in terms of carrying capacity shall be determined by the computation of stress based on authentic records of the design, details, materials, workmanship and physical condition, including data obtained by inspection (and tests if the records are not complete)." Rating calculations were based on the available structure drawings.

#### 3.1 AMTRAK BRIDGE 155.85 OVER THE USQUEPAUG RIVER IN RHODE ISLAND

For illustrative purposes, rating calculations were performed for an existing bridge. The bridge rated was Amtrak Bridge 155.85 over the Usquepaug River, Rhode Island, in Amtrak's Northeast Corridor. It is also the structure used for the field verification of the dynamic load model. The structure is on tangent track and supports trains travelling up to 150 mph. The bridge is a steel plate girder ballasted deck structure, simply supported on a center masonry pier and two abutments. The existing bridge was originally designed in 1905 for the New York, New Haven and Hartford Railroad (N.Y. N.H. & H. R.R.) and had its original spans replaced with steel riveted plate girders (open deck) fabricated between the 1920s and the 1930s. In 1993, a precast reinforced concrete deck was placed on the plate girders. The bridge now supports a track structure consisting of ballast, 136 RE Continuous Welded Rail, and 782 lb concrete ties.

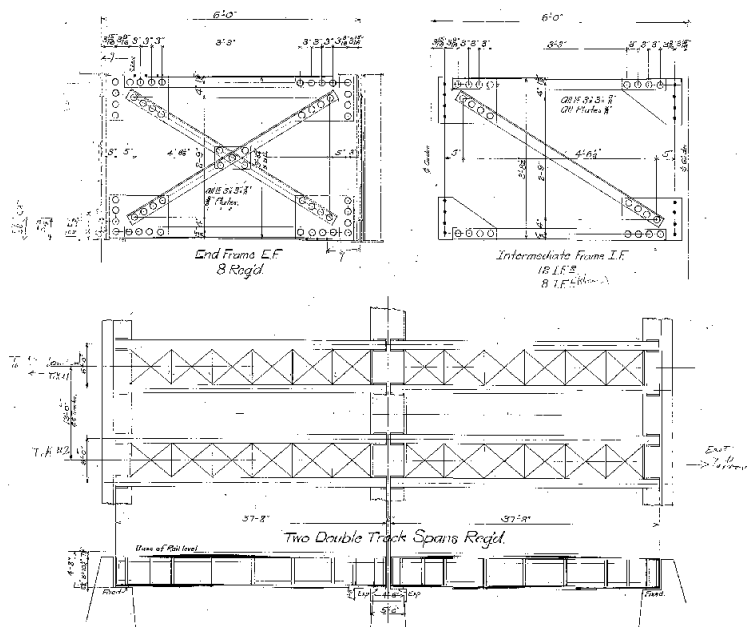


FIGURE 3.1 Span details of elevation, plan, and section views (N.Y. N.H. & H.R.R.).

### 3.2 NORMAL RATING CALCULATIONS

Normal rating calculations are based on bending and shear stresses in the girders that reflect Amtrak's Rating Policy, AREMA's MRE, and the original bridge plans. Since the actual date of the plans is unknown the yield stress of steel will be taken at  $F_y = 30,000$  psi. Detailed calculations can be found in the appendix at the end of the report, with a brief summary of the computations shown in this section. Bending (moment capacity) calculations are summarized below.

Impact load due to Vertical Effects (VE) is a percentage of live load. For rolling equipment and spans less than 80 feet, the AREMA equation is:

$$VE = 40 - \frac{3L^2}{1600}$$
$$VE = 37.57\%$$

where  $L = 36$  feet (CL of bearing to CL of bearing)

The impact load due to rocking effect (RE) is the vertical force couple, each being 20 percent of the wheel load without impact, acting downward on one rail and upward on the other.

$$RE = \frac{100}{S}$$
$$RE = 16.67\%$$

where  $S = 6$  feet (girder spacing)

Impact value for a ballasted deck is:

$$\text{Impact} = \frac{0.9(RE \pm VE)}{100} = 0.49$$

Live load moment capacity of girder is:

$$M_{LL} = \frac{M_{\text{avail}}}{1 + \text{Impact}} = 1,309.5 \text{ ft} - k$$

Cooper equivalent of one kip:

$$E_1 = \frac{1097.3 \text{ ft} - k}{80} = 13.716$$

The girder rating for bending is:

$$E_{\text{Cooper}} = \frac{M_{LL}}{E_1} = E95$$

The E95 rating for the bridge is based on an empirical impact calculation applied to a static load for speeds up to 90 mph. Once speeds exceed the 90 mph criteria, a moving load model can be applied to calculate the unknown impact values.

## 4 DETERMINATION OF DYNAMIC VERTICAL EFFECTS

The dynamic modeling computes impact values based on dynamic parameters that can be applied as a percentage of the static live load. A moving force model was used to analyze Bridge 155.85 and two sample bridge lengths for speeds between 50 mph and 250 mph. The model uses the same wheel spacing for each scenario since the equipment consist does not change for this territory. Natural frequencies and damping values do vary with each bridge and are estimated based on empirical formulas developed by Fryba (1996).

Note that the proposed model does not consider all of the potential factors affecting impact. Some of the neglected factors include the interaction of the structure with the suspension system of the train and direct consideration of the mass and inertial effects of the train load. These simplifying assumptions follow the procedure given in the Eurocode; however, the code does account for this interaction by increasing the damping coefficient to the moving load model. This same procedure is used to account for bridge–vehicle interaction effects within the model.

It is not customary within the high-speed rail industry to include vehicle–bridge interaction calculations to determine impact values. Wang states the moving load problem can be regarded as a special case of the more general formulation that considers the various dynamic properties of the moving vehicles. The moving load model is the simplest model that can be conceived, which has been frequently adopted by researchers in studying the vehicle-induced bridge vibrations. With this model, the essential dynamic characteristics of the bridge caused by the moving action of the vehicle can be captured with a sufficient degree of accuracy.

#### 4.1 MODELING

When developing the base line model, the input values, boundary conditions, and solutions were compared with measurements taken in the field for Bridge 155.85. The model is calibrated to a first natural frequency of 11.5 hertz, damping ratio of 3.58% (or 0.23 logarithmic decrement of damping), coach car , wheel spacing of 87 feet-6 in., and train speeds of 121 mph and 145 mph.

#### 4.2 DYNAMIC EQUATIONS AND CALCULATION SOFTWARE

The dynamic equations used in the calculations reflect commonly used theories and computations for varying spaced loads moving across a simply supported beam. The exact solutions to the equations of motion were used at time step intervals for the respective axle configuration. The calculations for the model were performed using Mathcad version 15 and Microsoft Excel 2010 software.

##### 4.2.1 The Moving Load Model

In many cases, especially when the vehicle to bridge mass ratio is small, the elastic and inertial effects of the vehicles may be ignored and much simpler models can be adopted for the vehicles. One typical example is the simulation of a moving vehicle over a bridge as a single moving load, which has been conventionally referred to as the moving load model (Yang 2004).

The Eurocode provisions for high-speed railroad bridge design indicate in Section 6.4.6.4—Modeling the Excitation and Dynamic Behavior of the Structure (1), the dynamic effects of a real train may be represented by a series of moving point forces. Vehicle/structure mass interaction effects may be neglected and for spans of less than 30 m dynamic vehicle/bridge mass interaction tends to reduce the peak response at resonance (Eurocode 1 Part 2).

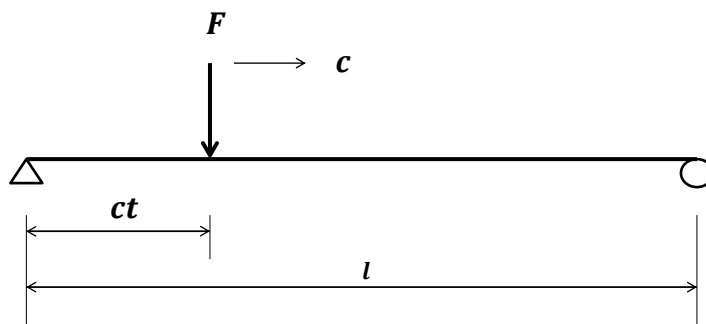


FIGURE 4.1 Motion of a constant force  $F$  along a simply supported beam of span  $l$  at velocity  $c$ .

The partial differential equation of motion can be established for a simply supported span of constant mass and stiffness from vertical force equilibrium and bending moments in a beam element as:

$$EI \frac{\partial^4 v(x, t)}{\partial x^4} + \mu \frac{\partial^2 v(x, t)}{\partial t^2} + 2\mu\omega_b \frac{\partial v(x, t)}{\partial t} = \delta(x - ct)F$$

$v(x, t)$  Displacement in the direction of the  $y$  axis  
 $x$  coordinate in the direction of the  $x$  axis  
 $t$  time  
 $c$  motion velocity (velocity of force along the  $x$  axis)  
 $F$  Force  
 $l$  Length  
 $E$  Modulus of Elasticity  
 $I$  Inertia  
 $\mu$  mass per unit length of a beam  
 $\omega_b$  circular frequency with damping

The exact solution to the motion of a constant  $F$  along a simply supported beam is:

$$v(x, t) = v_0 \sum_{j=1}^{\infty} \frac{1}{j^2 [j^2 (j^2 - \alpha^2)^2 + 4\alpha^2 \beta^2]} \cdot \left[ j^2 (j^2 - \alpha^2) \sin j\omega t - \frac{j\alpha [j^2 (j^2 - \alpha^2) - 2\beta^2]}{(j^4 - \beta^2)^{1/2}} e^{-\omega_b t} \cdot \sin \omega_j' t - 2j\alpha\beta (\cos j\omega t - e^{-\omega_b t} \cos \omega_j' t) \right] \sin \frac{j\pi x}{l}$$

Static deflection of the beam at midspan due to force  $F$  applied at the same point:

$$v_0 = \frac{2F}{\mu l \omega_j^2} = \frac{2Fl^3}{\pi^4 EI}$$

Dimensionless velocity (speed) parameter:

$$\alpha = \frac{\omega}{\omega_1} = \frac{c}{2f_1 l}$$

Dimensionless damping parameter (damping ratio):

$$\beta = \frac{\omega_b}{\omega_1} = \frac{\vartheta}{2\pi}$$

Circular frequency of force passage:

$$\omega = \frac{\pi c}{l}$$

Circular frequency of damped vibrations of unloaded beam at subcritical damping ( $\omega_b < \omega_j$ ):

$$\omega_j'^2 = \omega_j^2 - \omega_b^2$$

Circular frequency of undamped vibrations of unloaded simply supported beam:

$$\omega_j^2 = \frac{j^4 \pi^4 EI}{l^4 \mu}, \quad f_i = \frac{\omega_j}{2\pi}$$

Natural circular frequency of the system:

$$\omega_0 = \left(\frac{k}{m}\right)^{1/2}$$

Natural frequency of a simply supported beam:

$$\omega_1 = \pi^2 \sqrt{\frac{EI}{\mu l^4}}$$

Logarithmic decrement of damping on the basis of  $n$  successive vibrations where  $s_n$  is the amplitude after the  $n$ th cycle:

$$\vartheta = \frac{1}{n} \ln \frac{s_0}{s_n}$$

Logarithmic decrement of damping to the constant:

$$\vartheta = \frac{\omega_b}{f_d}$$

Speed parameter:

$$\alpha = \frac{\pi C}{\omega L}$$

Mode of vibration (1<sup>st</sup> Mode is to be used):

$$j = 1, 2, 3 \dots$$

#### 4.2.2 Natural Frequency and Damping Equations

The most important dynamic characteristic of a railway bridge is its natural frequency, which characterizes the extent to which the bridge is sensitive to dynamic loads (Fryba 1999). Moving force loads at different frequencies excite the structural system if the velocities are close to the structure's natural frequency.

Natural frequency of a simply supported beam:

$$\omega_1 = \pi^2 \sqrt{\frac{EI}{\mu l^4}}$$

$$f_1 = \frac{\omega_1}{2\pi}$$

Plate girder bridge with ballast—First natural frequency empirical equation (Fryba1996):

$$f_1 = 59 \left( \frac{l}{3.28} \right)^{-0.7}$$

Comparisons of Bridge 155.85's natural frequency based on equations and field data:

Bridge 155.85 Natural Frequency Values		
Natural Frequency for a Simply Supported Beam	Field Observation Value	Empirical Equation for a Plate Girder Bridge with Ballast
11.5 Hz	12 Hz	11 Hz

Logarithmic decrement of damping (Fryba 1996) for steel bridges < 65 feet :

$$\vartheta = 0.08 \left( 65.62/l \right)^{1.5}$$

#### 4.2.3 Moving Load Model with Vehicle–Bridge Interaction Considerations

Accounting for vehicle–bridge mass interaction effects may be accomplished by increasing the value of damping assumed for a structure by Equation 6.13 (Eurocode).

Damping equations  $\beta$  (damping ratio) and  $\vartheta$  (Logarithmic decrement of damping):

$$\beta = \frac{\omega_b}{\omega_1} = \frac{\vartheta}{2\pi}$$

$$\vartheta = \frac{\omega_b}{f_d}$$

Additional damping  $\Delta\beta$  from Equation 6.13 (Eurocode) as a function of span length  $l$  is given by:

$$\beta_{\text{TOTAL}} = \beta + \Delta\beta$$

$$\Delta\beta = \frac{0.0187 \left( \frac{l}{3.28} \right) - 0.00064 \left( \frac{l}{3.28} \right)^2}{1 - 0.0441 \left( \frac{l}{3.28} \right) - 0.0044 \left( \frac{l}{3.28} \right)^2 + 0.000255 \left( \frac{l}{3.28} \right)^2} [\%]$$

For Bridge 155.85, the calculation is:

$$\beta_{\text{TOTAL}} = 3.18\% + 0.40\%$$

$$= 3.58\%$$

$$\vartheta = 0.23$$

#### 4.2.4 Wheel Load Case

This type of model scenario takes into account the wheel loads from the power and coach cars entering and leaving the beam. Since Amtrak inspects its track at regular intervals, the loads entering and leaving the bridge were analyzed according to these conditions. In general, the rail irregularities have little influence on the impact response of the bridges. However, the same is not true with the moving vehicles or sprung masses (Wang). The terms  $P_n(c, t) + P_n(c, t - t_c)$  represent the dynamic response excited by wheel loads following one another of the train consist, with the following wheel having a time lag  $t_c$ . The terms A and B on page 10 represent the same wheel load entering and leaving the beam, respectively.

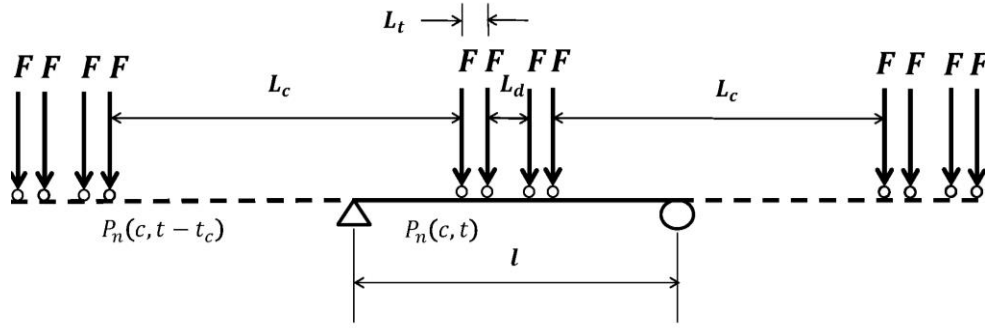


**FIGURE 4.2 Load configuration.**

$F$  is the resultant wheel load applied at the axle  
 $L_c$  is the distance between the front and rear wheels of the car  
 $L_t$  is the distance between the wheels within the truck assembly  
 $L_d$  is the distance between the wheels of the coupler.

$P_n(c, t)$  = Dynamic response excited by the initial wheel  
 $P_n(c, t - t_c)$  = Dynamic response excited by the following wheel.

Vertical deflection:

$$v(x, t) = \sum_{n=1}^{\infty} q_n(t) \sin \frac{n\pi x}{l}$$

Vertical coordinate:

$$q_n(t) = \frac{2pl^3}{EI\pi^4} [P_n(c, t) + P_n(c, t - t_c)]$$

Bending moment:

$$M(x, t) = \sum_{n=1}^{\infty} qm_n(t) \sin \frac{n\pi x}{l}$$

Bending moment coordinate:

$$qm_n(t) = \frac{2pl}{\pi^2} [P_n(c, t) + P_n(c, t - t_c)]$$

Dynamic response excited by the front wheel:

$$P_n(c, t) = \sum_{k=1}^N \frac{1}{(1 - \alpha^2)^2 + 4(\beta\alpha)^2} \left[ A \cdot H(t - t_k) + (-1)^{n+1} B \cdot H\left(t - t_k - \frac{l}{c}\right) \right]$$



$$A = \left[ j^2 (j^2 - \alpha^2) \sin j\omega(t - t_k) - \frac{j\alpha[j^2(j^2 - \alpha^2) - 2\beta^2]}{(j^4 - \beta^2)^{1/2}} e^{-\omega_b(t-t_k)} \cdot \sin \omega_j(t - t_k) \right. \\ \left. - 2j\alpha\beta(\cos j\omega(t - t_k) - e^{-\omega_b(t-t_k)} \cos \omega_j(t - t_k)) \right]$$

$$B = \left[ j^2 (j^2 - \alpha^2) \sin j\omega\left(t - t_k - \frac{l}{c}\right) - \frac{j\alpha[j^2(j^2 - \alpha^2) - 2\beta^2]}{(j^4 - \beta^2)^{1/2}} e^{-\omega_b(t-t_k-\frac{l}{c})} \cdot \sin \omega_j\left(t - t_k - \frac{l}{c}\right) \right. \\ \left. - 2j\alpha\beta\left(\cos j\omega t - e^{-\omega_b(t-t_k-\frac{l}{c})} \cos \omega_j\left(t - t_k - \frac{l}{c}\right)\right) \right]$$

- $t_k$  time for load to appear at beam  
 $\frac{l}{c}$  time for load to cross beam  
 $A$  load entering beam  
 $B$  load leaving beam.

### 4.3 MODEL AND FIELD RESULTS

As previously noted, field monitoring of Bridge 155.85 was performed to compare and verify the model output. Several revenue trains and one work train were monitored during this period. The model results reported below were selected to match the train consists and speeds of the actual trains monitored at the bridge. Deflection comparisons (between model results and field measurements) are shown for several trains later in this report.

#### 4.3.1 Model Verification

Four model comparisons were made to girder deflection field results reflective of two Amtrak train consists moving at different speeds. The first, a working train, was used to obtain static and dynamic load information applicable to the basic model input. The second, an Acela train travelling at 120 and 145 mph, was used to verify dynamic effects of an actual high-speed rail train. The axle spacing and weights of the two train consists are significantly different and provide a broad range of data to help reinforce the model verification. Comparisons between the model and field data were achieved by examination of the deflection and strain results with respect to time. A graph of the model results superimposed on the field data can be found in Figures 5.3–5.6

The graphs that follow illustrate modeled deflection results for the working train, and two separate graphs representing deflection and bending moments for Amtrak's Acela train consist.

#### 4.3.2 Work Train Model Information

The two graphs represent a working train model consisting of a coupled GP 38 and MP 15 locomotives moving across the 36 foot girder at 6 and 41 mph. The first graph is considered a quasi-static load model and can be used to provide a static load envelope for the axle configuration. The second model illustrates the dynamic response of the girder from the train passing across the bridge at 41 mph.

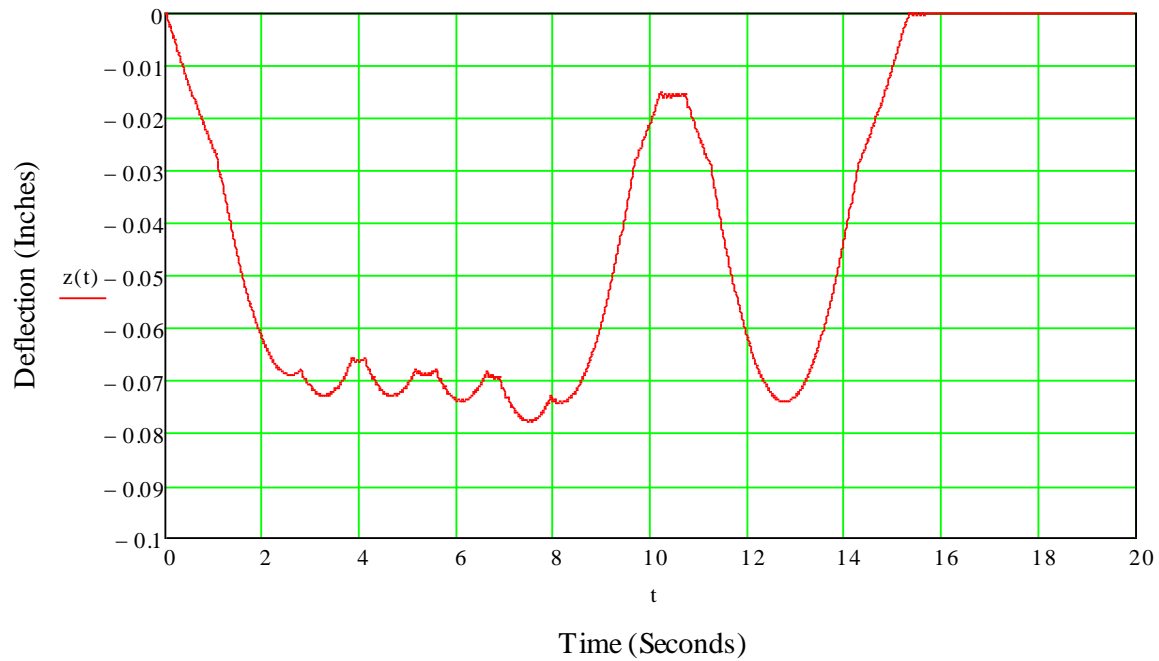


**FIGURE 4.3 Six mph train speed induced girder deflections at midspan.**

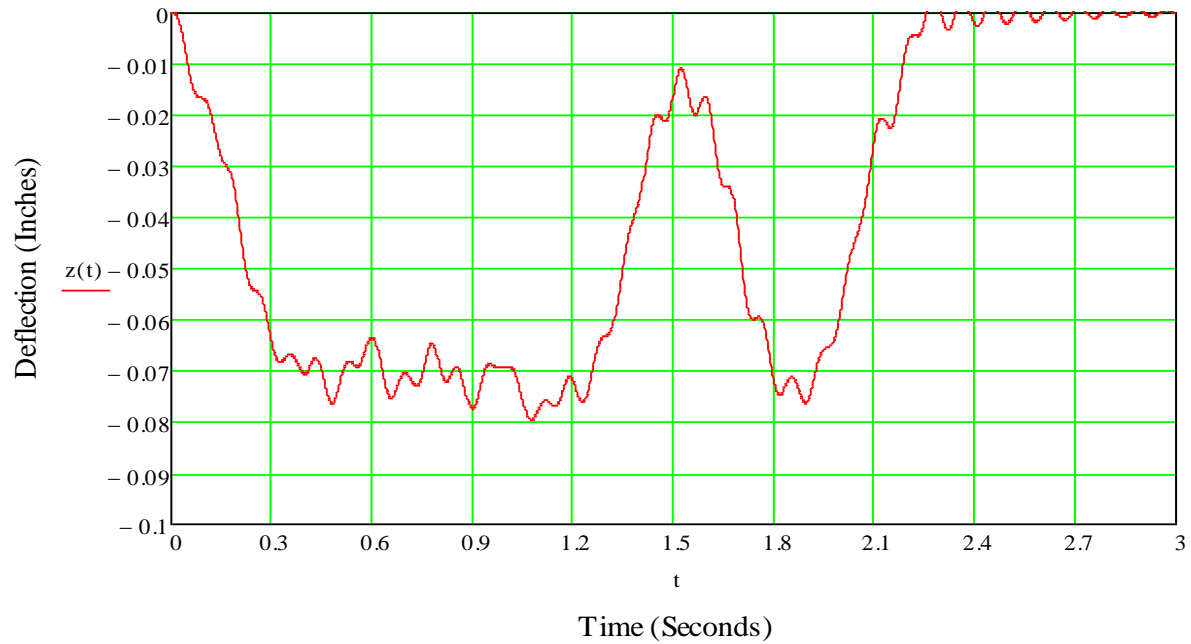


**FIGURE 4.4 Forty-one mph train speed induced girder deflections at midspan.**

### 4.3.3 Acela Train Model Information

Two graphs are created for each train speed representing girder deflections (serviceability) and bending moment (strength) values. The following two graphs are quasi-static load models and the graphs found on pages 20 and 21 represent Acela trainsets for 120 and 145 mph. The graphs can be used to calculate both deflection ratios and bridge ratings. Additionally, figures 4.11 to 4.14 reflect girder responses superimposed on the quasi-static load condition.

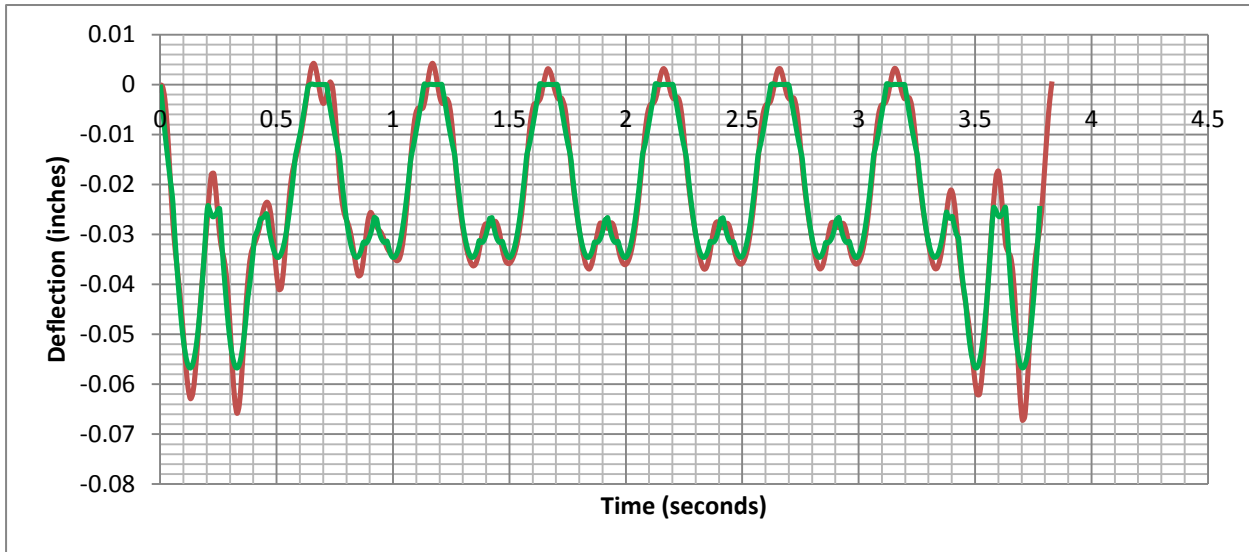


**FIGURE 4.5** One-hundred and twenty mph train speed induced girder deflections at midspan superimposed on the quasi-static 6 mph train.

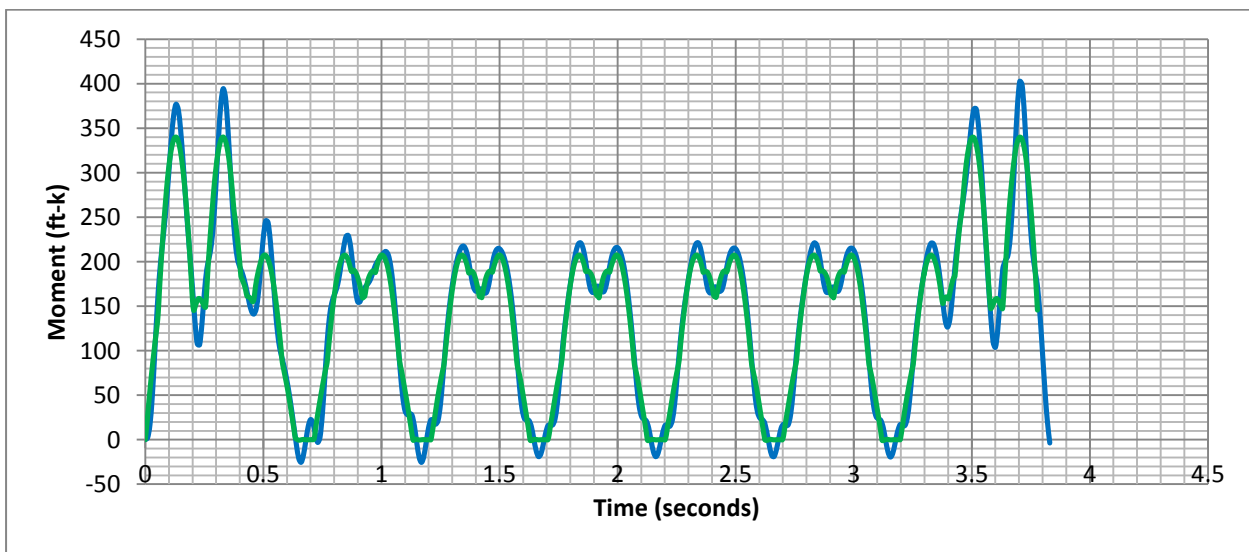


**FIGURE 4.6** One-hundred and twenty mph train speed induced girder bending moments at midspan superimposed on the quasi-static 6 mph train.

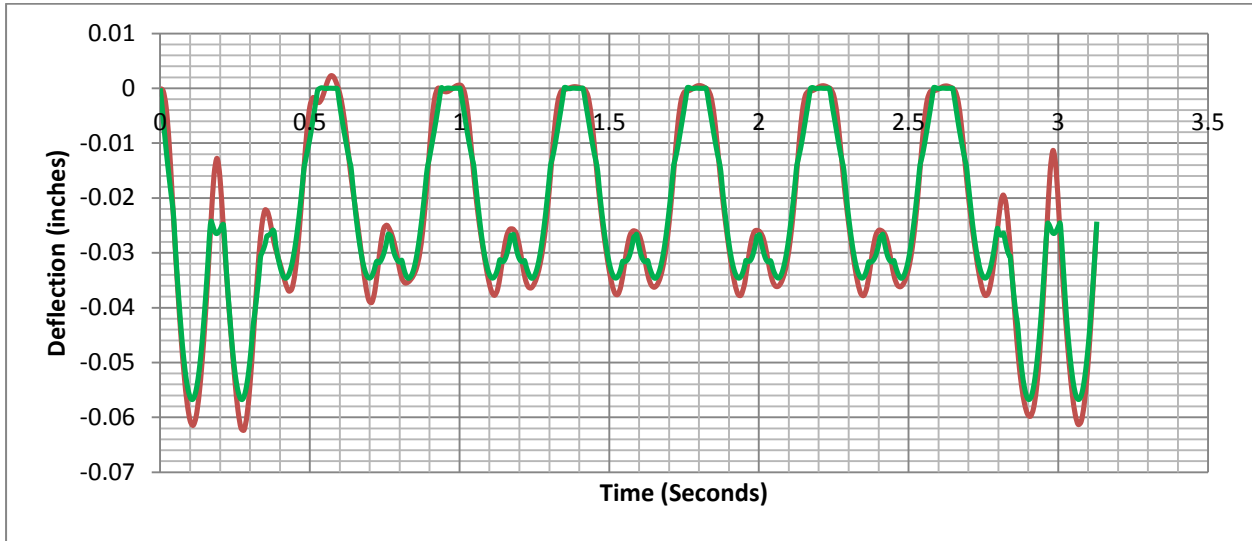


**FIGURE 4.7 One-hundred and forty-five mph train speed induced girder deflections at midspan superimposed on the quasi-static 6 mph train.**

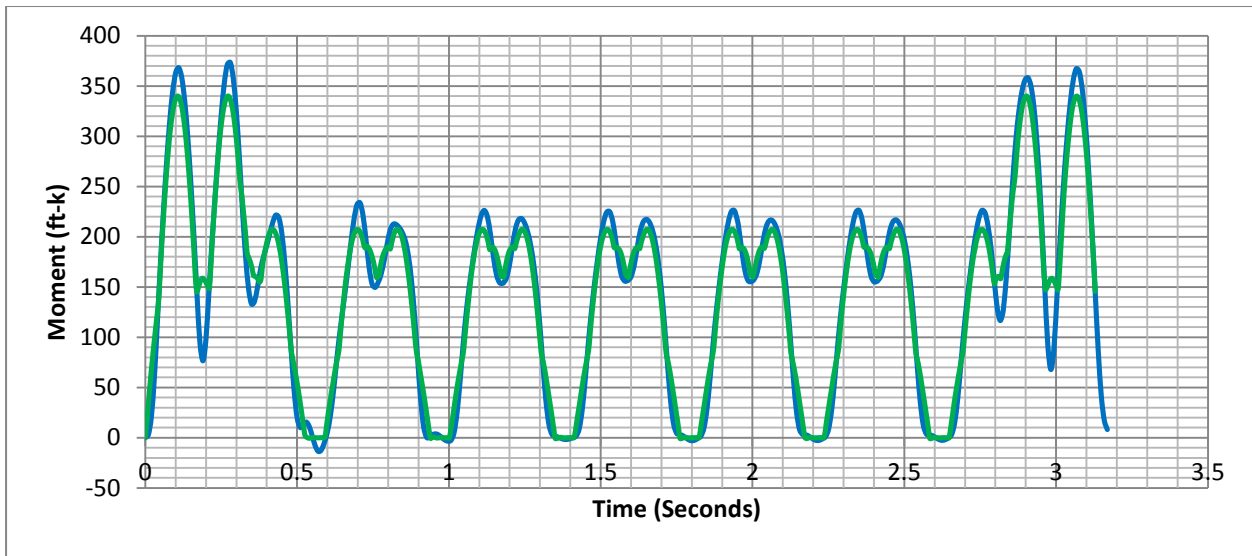


**FIGURE 4.8 One-hundred and forty-five mph train speed induced girder bending moments at midspan superimposed on the quasi-static 6 mph train.**

#### 4.3.4 Byers Report

The 1970 article “Impact from Railway Loading on Steel Girder Span” prepared by William Byers, provides a table that illustrates some of the impact values associated with several types of bridges, various train speeds, and different bridge lengths. Examination of “Table 1—Summary of Tests,” shows increasing impact values as speed increases over lower speed ranges. However, the observed impact values reduce over the highest range of speeds (80–100 mph). This could represent a resonant speed observed from data taken back in 1970 and is reflected for all bridge lengths. In addition, the values from the model are consistent with the impact values shown in the table for a ballast deck span.

TABLE 4.1 Comparison of Impact Values Between the Byers Report and Mathematical Modeling

Speed Range (mph)	Impact Values for Various Speed Ranges		
	60-80	70-90	80-100
Byers Report	12.7	14.8	13
Modeling	11-18	11-24	12-27

1100

July, 1970

ST 6

TABLE 1.—SUMMARY OF TESTS

Span length range, in feet (1)	Speed range, in miles per hour (2)	Number of test runs (3)	Number of spans tested (4)	Mean percent impact (5)	Coefficient of variation for impact (6)
(a) Ballast Deck Spans					
30 to 60	0-20	17	5	7.2	0.89
	10-30	11	4	10.0	0.64
	20-40	22	4	9.0	0.59
	30-50	32	5	10.5	0.67
	40-60	33	5	10.9	0.84
	50-70	31	5	14.0	0.44
	60-80	36	5	12.7	0.68
	70-90	31	5	14.8	0.47
	80-100	20	5	13.0	0.52
60 to 90	0-20	40	9	5.4	1.00
	10-30	33	9	7.8	0.56
	20-40	43	9	7.0	1.26
	30-50	69	9	11.0	0.67
	40-60	80	9	10.0	0.90
	50-70	67	9	12.7	0.50
	60-80	65	8	13.0	0.60
	70-90	74	8	14.0	0.61
	80-100	57	8	12.5	0.75
90 to 140	0-20	18	4	6.0	1.07
	10-30	22	4	8.3	0.49
	20-40	39	4	8.8	0.50
	30-50	56	4	6.2	1.23
	40-60	45	4	6.6	1.23
	50-70	32	4	11.7	0.68
	60-80	17	3	10.4	1.17
	70-90	8	2	19.6	0.48
	80-100	17	2	17.0	0.50

FIGURE 4.9 Page 1100 of the Byers report illustrating mean percent impact values.

#### 4.4 RESONANT SPEEDS

A system acted upon by an external excitation of frequency coinciding with the natural frequency of the span is said to be at resonance. Given the car length of  $d$  and simple span length  $l$  the speed parameter  $\alpha$  can be found from the resonance condition as:

$$\alpha_i = \frac{d}{2il}, \quad i = 1, 2, 3 \dots$$

$$\alpha = \frac{c_i}{2f_1 l}$$

By inserting the  $i$  values into the equation, the primary resonance occurs at  $0.5 d/l$ , and the secondary resonances occur at  $0.25 d/l$ ,  $0.167 d/l$ , and  $0.125 d/l$ . The calculated resonance speeds for the range of velocities to be reviewed will establish the peak impact factors for that given range.

The resonant speeds can also be estimated as:

$$c_i = n_0 \lambda_i$$

where:

$c_i$  = resonant speed

$n_0$  = first natural frequency of the unloaded bridge

$\lambda_i$  = principle wavelength of frequency of excitation

$$\lambda_i = \frac{d}{i}$$

$d$  = regular spacing of groups of axles

$i = 1, 2, 3 \dots$

#### 4.5 CANCELLATION

Cancellation occurs if the time lag between loads crossing the span equals an odd multiple of the half period  $\frac{1}{2}(\frac{2\pi}{\omega})$ . In this case, the wave components induced by the sequentially moving loads will cancel out. An optimal train speed can be selected to produce cancellation for a particular span length. This will produce the most desirable riding condition.

$$\alpha_i = \frac{1}{2i - 1}, \quad i = 1, 2, 3 \dots$$

$$\alpha = \frac{c_i}{2f_1 l}$$

#### 4.6 DYNAMIC VERTICAL EFFECT (DVE)

The DVE is based on the following equation, comparing maximum dynamic stresses or deflections at midspan with the static condition.

$$DVE = \frac{v_d(x) - v_s(x)}{v_s(x)}$$

$DVE$  = Dynamic Vertical Effect (Impact) for stress or deflection

$v_d(x)$  = dynamic stress or deflection at midspan

$v_s(x)$  = static stress or deflection at midspan.

## 5 FIELD TESTING

### 5.1 OVERVIEW

The monitoring effort was directed by Gary T. Fry, Ph.D. Dr. Fry has extensive experience in instrumentation and monitoring of railroad bridges. Dr. Fry was assisted by W.N. Marianos, Jr., Ph.D., and Carlos Puerto. The instrumentation and testing were conducted on November 21 and 22, 2013. The weather was overcast on November 21, with steady drizzle and rain on November 22. The temperature was in the 30s both days.

Mr. Kevin Bollinger, project manager for Hatch Mott MacDonald, was on-site through the monitoring process. On-track safety was provided by Amtrak watchmen/flaggers. General assistance was provided by Amtrak Bridge and Building Department personnel. Mr. Craig Rolwood, Project Director, Structures Design for Amtrak, was on-site for the monitoring as well.

### 5.2 BRIDGE DESCRIPTION

Bridge 155.85 is a two-span structure crossing the Usquepaug River. The spans are steel deck plate girders with precast concrete ballast deck panels. The deck plate girders are riveted spans fabricated prior to 1933. According to the bridge plans, the deck panels were added around 1993.

Two railroad tracks cross the river at this site. Separate structures carry the eastbound and westbound tracks.



**FIGURE 5.1 Amtrak Bridge 155.85.**

The bridge was selected for monitoring by Amtrak, in coordination with Hatch Mott MacDonald personnel. It is considered to be representative of a number of spans on the Northeast Corridor high-speed rail line.

### 5.3 INSTRUMENTATION DESCRIPTION

The two spans carrying the westbound track were instrumented. The instrumentation included six string potentiometers (Celesco model SM2) per span for checking deflections. Potentiometers were located at the midspan and each bearing of each plate girder. Potentiometers were mounted to fixed points on the bridge substructure (or on frames at midspan) and connected to the bottom of the bridge girders. Two strain gauges were placed at midspan of each plate girder, on the girder webs above the top of the bottom flange angle and below the bottom of the top flange angle.



**FIGURE 5.2 String potentiometer mounted near girder bearing.**

Data were collected using an electronic data acquisition system. Data acquisition was controlled using Daisylab software on a laptop computer. The monitoring instruments were connected to the data acquisition system by cables. The system was powered by a generator provided by Amtrak.

### 5.4 MONITORING PROCEDURE

Data were collected during the passage of seven regularly scheduled passenger trains. In addition, Amtrak provided a test train consisting of two locomotives. The test train crossed the bridge, stopping at specified locations to allow collecting data on bridge performance under a known loading. In addition, the test train crossed the bridge at 5, 10, 30, and 40 mph speeds for the collection of dynamic data.



### 5.4.1 TRAINS MONITORED

The information on the following page was provided by Amtrak personnel.

**November 21, 2013**

Passenger Train:

Time	Train #	Direction
10:48 p.m.	67	Westbound

**November 22, 2013**

Work Train

MP15 and GP38 locomotives (MP15 ahead on westbound track).

Passenger Trains:

Time	Train #	Direction	Power Car	Coaches
10:05 a.m.	2159	Westbound	2 Acela PC	6 Acela Coaches
10:37 a.m.	83	Westbound	P42 & AEM-7	8-Amfleet I
12:06 p.m.	2163	Westbound	2 Acela PC	6 Acela Coaches
12:16 p.m.	173	Westbound	AEM-7	8-Amfleet I
1:05 p.m.	2165	Westbound	2 Acela PC	6 Acela Coaches
2:06 p.m.	2167	Westbound	2 Acela PC	6 Acela Coaches

Equipment Weights:

Vehicle	Weight	Wheelbase	Truck Centers	Passenger Capacity
GP38	264,000	9' 0"	32' 10"	
MP15	246,000	9' 0"	24' 2"	
Amfleet I Coach	110,000	8' 6"	59' 6"	72
AEM-7	201,500	9.66'	25' 7.06"	
HHP-8	223,000	35' 4"	35' 4"	
ACS-64	217,000	9' 10.1"	31' 9.1"	
Acela PC	203,000	9' 4"	35' 3"	
Acela Coach	125,000	9' 10"	59' 6"	64
P42	266,000	9' 0"	43' 2.5"	

Note that coach weights do not include passengers.

## 5.4.2 MONITORING RESULTS

The following charts show the calculated model results for several trains overlaid with the field measurements for these trains. The measurements compared are for midspan deflections. Note that since revenue trains could not be stopped on the bridge for static measurements, calculation of impact factors cannot be directly made from field measurements.

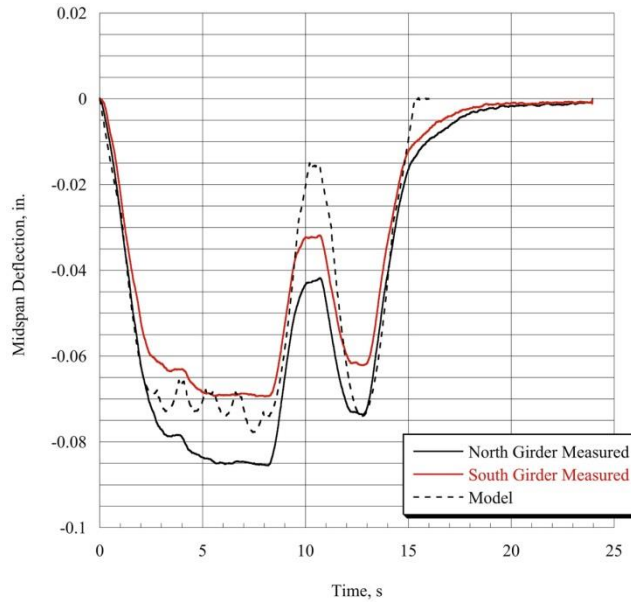


**FIGURE 5.3A Midspan deflection of east span girders (Amtrak work train, 6 mph).**

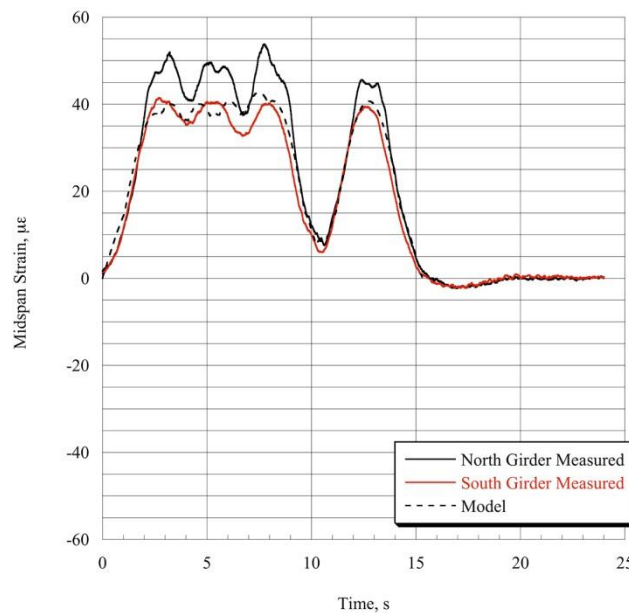


**FIGURE 5.3B Midspan strain of east span girders at lower strain gage location 16.125 in. below section centroid (Amtrak work train, 6 mph).**

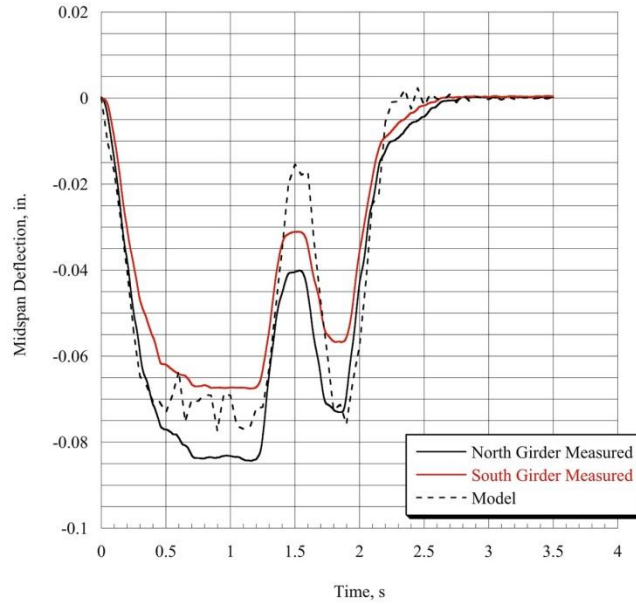


**FIGURE 5.4A Midspan deflection of east span girders (Amtrak work train, 41 mph).**

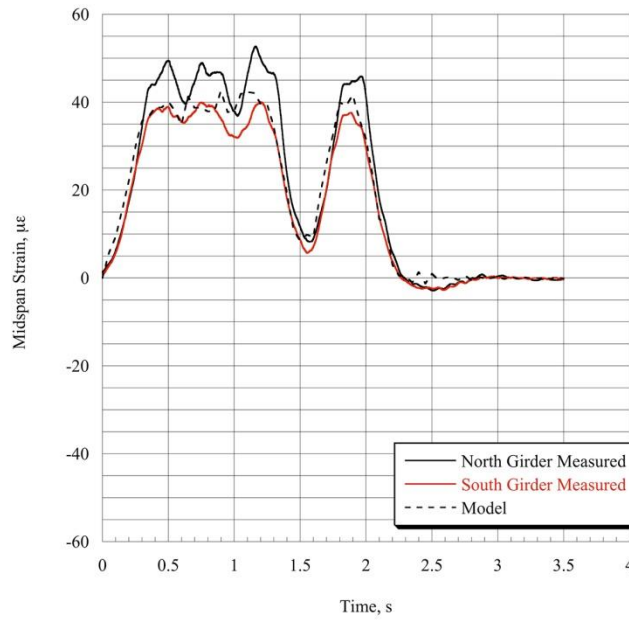


**FIGURE 5.4B Midspan strain of east span girders at lower strain gage location 16.125 in. below section centroid (Amtrak work train, 41 mph).**

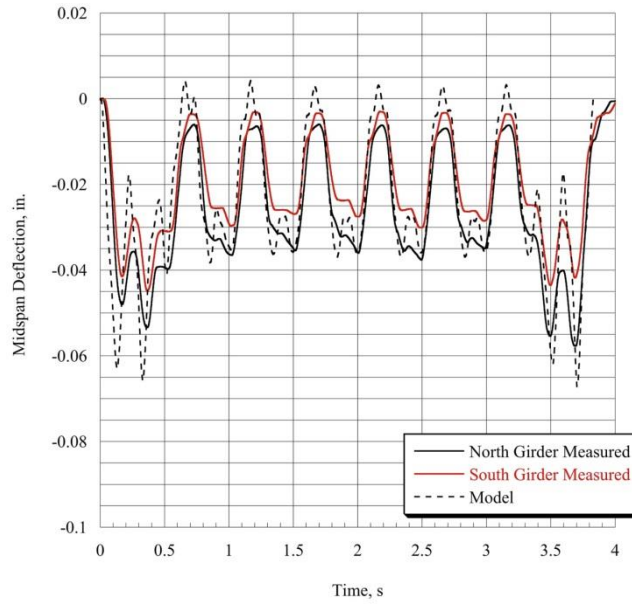


**FIGURE 5.5A** Midspan deflection of east span girders (Amtrak Acela train, 120 mph).

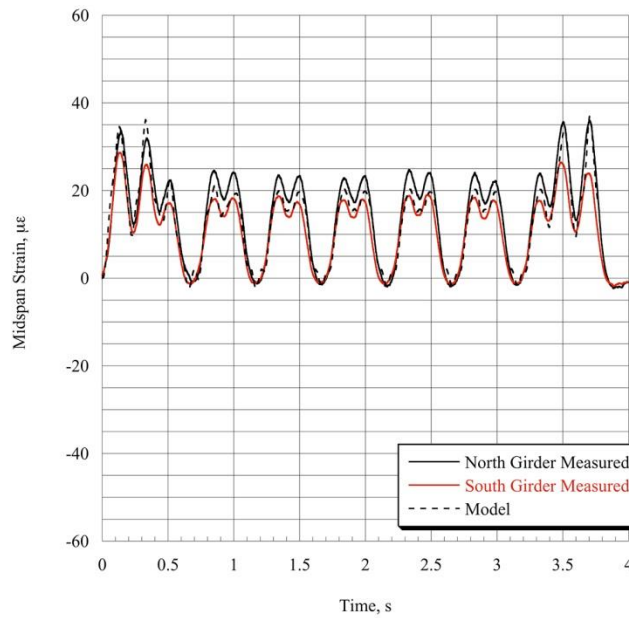


**FIGURE 5.5B** Midspan strain of east span girders at lower strain gage location 6.125 in. below section centroid (Amtrak Acela train, 120 mph).

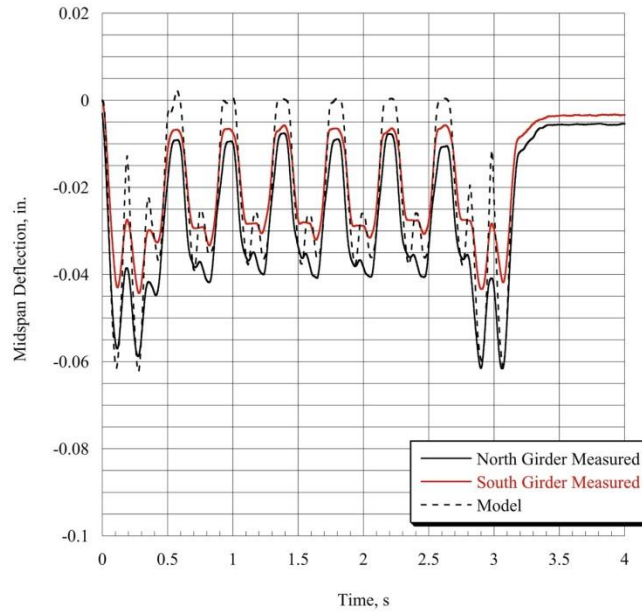


**FIGURE 5.6A** Midspan deflection of east span girders (Amtrak Acela train, 145 mph).

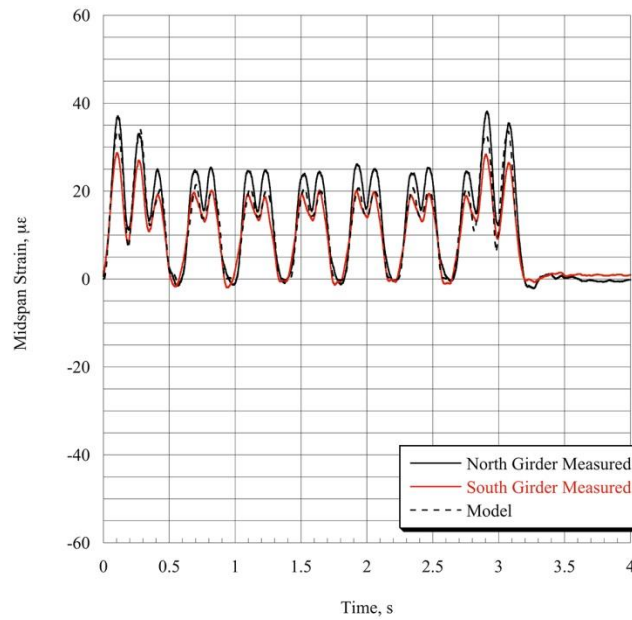


**FIGURE 5.6B** Midspan strain of east span girders at lower strain gage location 16.125 in. below section centroid (Amtrak Acela train, 145 mph).

## 6 PROPOSED RATING PROCEDURE

### 6.1 NORMAL RATINGS CONSIDERING DYNAMIC CHARACTERISTICS

Once a normal rating has been determined in accordance with the AREMA MRE and Amtrak’s Rating Policy, a dynamic normal rating can be determined by the equations and methodologies considered in this report. Results from the dynamic impact calculations can be compared with the vertical component of the current AREMA impact equation. The greater of the two vertical effect values will be used in calculating the normal rating. An illustration of the general procedure is given by the flow chart in Figure 6.1.

It should be noted that the procedure described is specifically for rating, not design, of new structures. Ratings are calculated for existing structures. Therefore, conditions that may affect the rating (such as structure deterioration and approach conditions) can be identified in the field and included in the structure evaluation. Because of this, the use of typical impact vertical effect values (instead of the worst conceivable case) is acceptable, particularly for normal ratings. It should also be noted that high-speed rail track structures and equipment are closely monitored, reducing the likelihood of high-impact values due to deterioration and damage of infrastructure and vehicles.

A complete normal rating calculation for Bridge 155.85 results in a rating controlled by AREMA criteria. However, the analysis for bridges with lower natural frequencies can result in high magnitude vertical effects at certain train speeds. In such cases, a detailed analysis would need to be computed because of track structure deterioration associated with high deck accelerations.

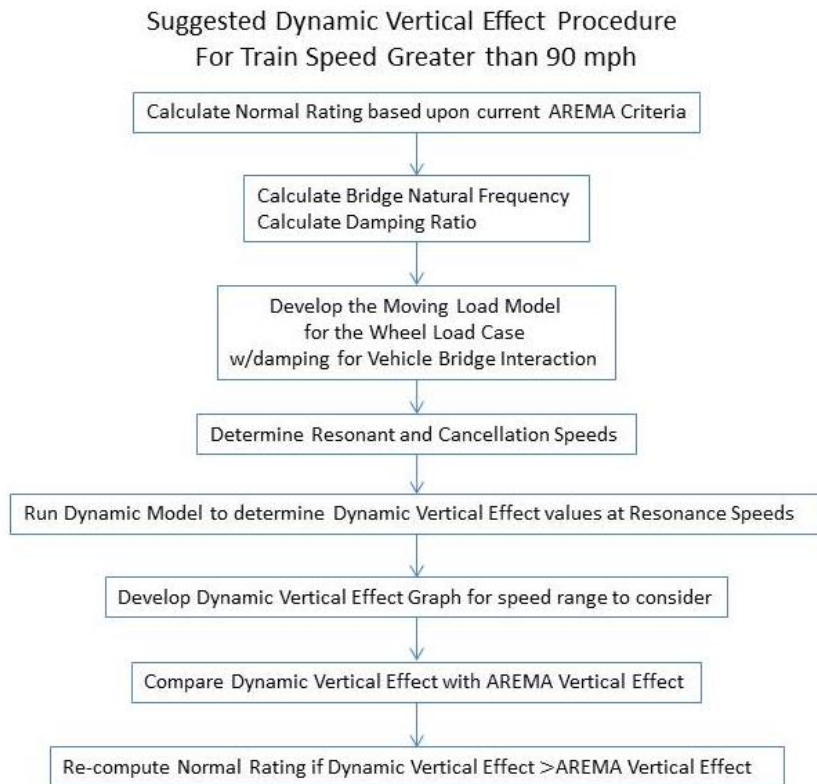


**FIGURE 6.1 Flow chart.**

**TABLE 6.1 Normal Bridge Ratings Summary for Br. 155.85**

	<b>AREMA Manual</b>	<b>Dynamic Analysis</b>
Vertical Effect	38%	27%
Cooper E Loading	E95	E102

## 7 BRIDGE LENGTH AND TRAIN SPEED COMPARISONS

### 7.1 COMPARISON OF BRIDGE LENGTHS

Figures 7.1–7.6 illustrate the dynamic vertical effect versus train speed for bridge span lengths of 15, 36, 60, 80, 100, and 150 feet. The orange line represents AREMA’s current vertical effect impact value limit for a 90 mph train (maximum train speed). The field observations recorded in November 2013 for bridge 155.85 compare well with the calculated deflection values for the 36-foot bridge length. The impact values associated with all the girder spans are also plotted for comparison. The dynamic vertical effect for each bridge length is calculated with different known bridge frequencies and damping for a ballasted steel girder bridge (Fryba 1999). The natural frequency and wheel spacing greatly influence the magnitude of the responses, and any final bridge evaluation needs to take into account calculated bridge natural frequencies.

Graphs representing span lengths 15, 60, and 80 feet illustrate coach car vertical effect values of 75% to 85%, and should be considered in the analysis of a bridge load rating. Even though the coach car is not as heavy as a power car, it has similar deflection values to that of a power car and need to be taken into consideration. These observations, which are significant, also demonstrate that the Coach Car Cooper E Equivalents associated with these impact values are below the normal loading rating of a typical E80 North American Railroad Bridge.

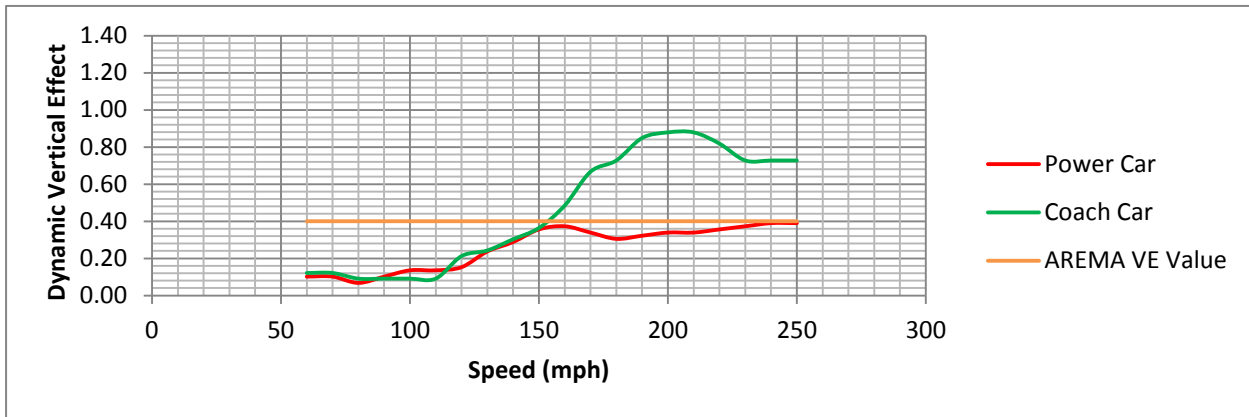


FIGURE 7.1 Dynamic vertical effects for a 15-foot span bridge.

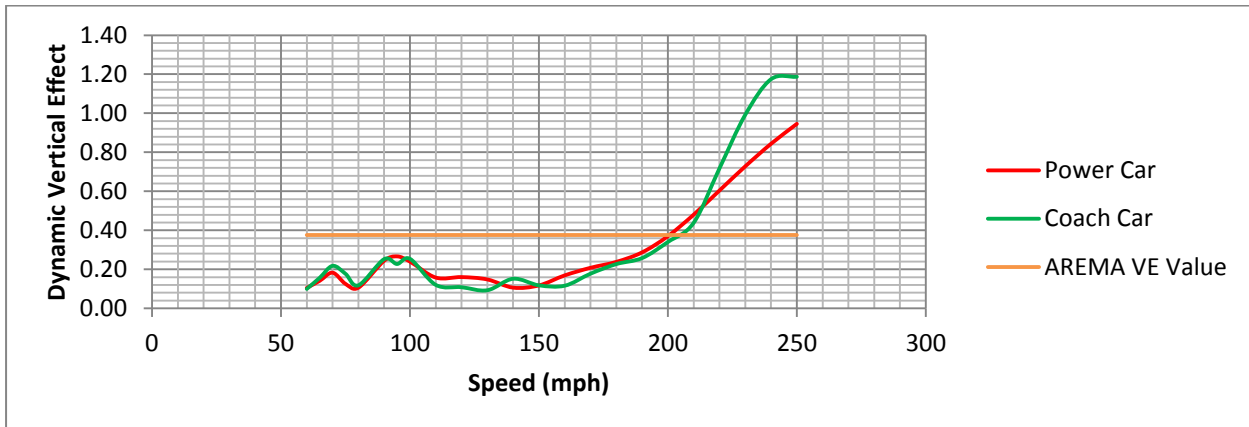


FIGURE 7.2 Dynamic vertical effects for Bridge 155.85 (36-foot span).

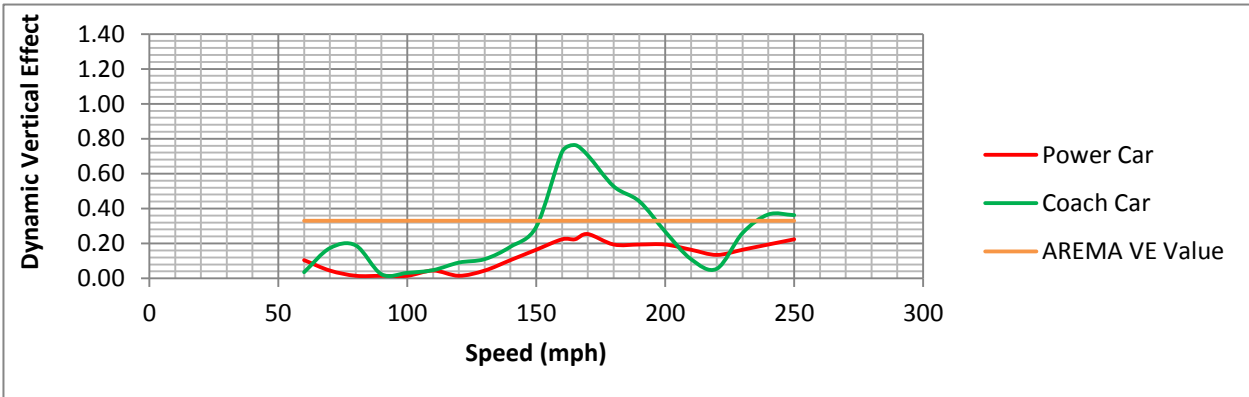


FIGURE 7.3 Dynamic vertical effects for a 60-foot span bridge.

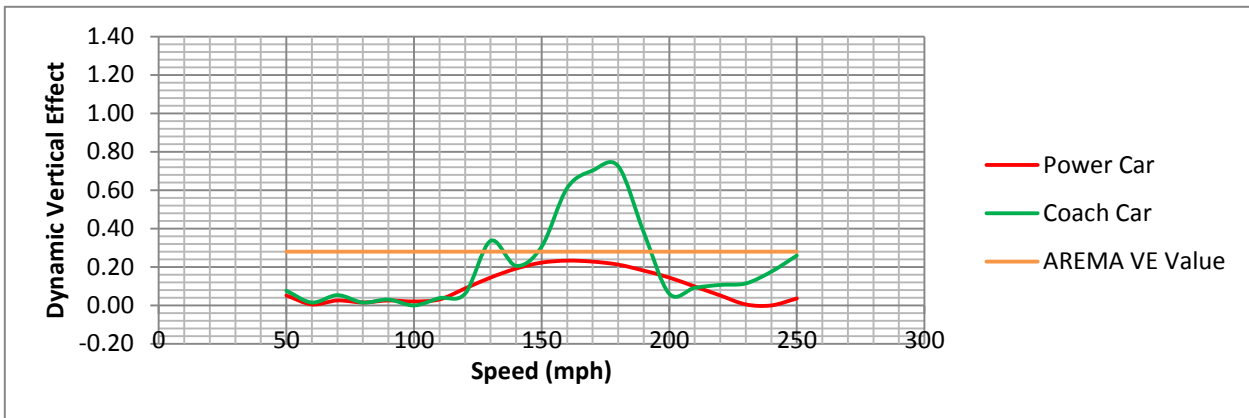


FIGURE 7.4 Dynamic vertical effects for an 80-foot span bridge.

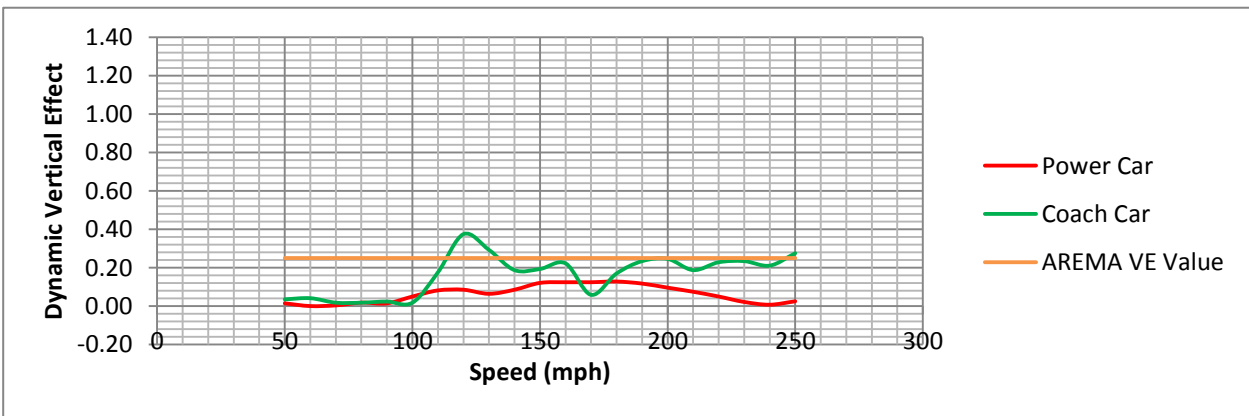
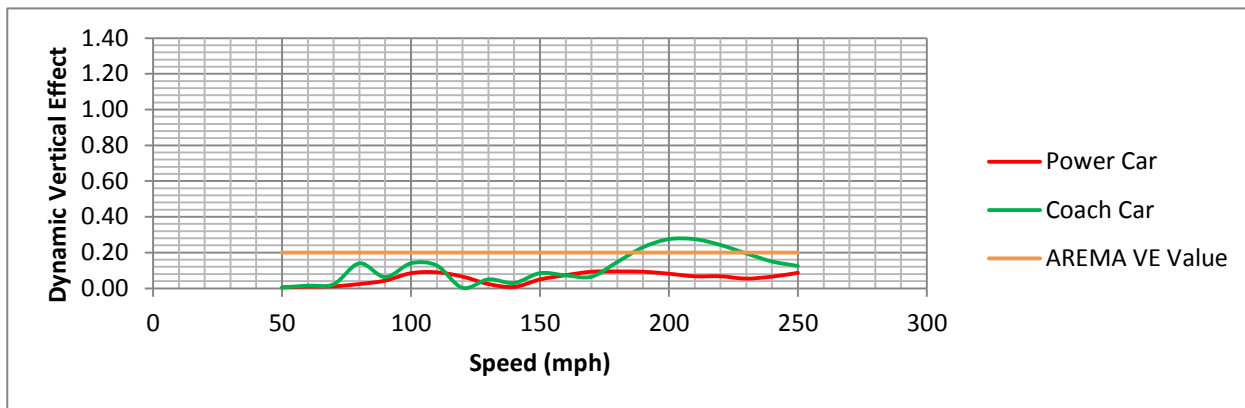


FIGURE 7.5 Dynamic vertical effects for a 100-foot span bridge.





**FIGURE 7.6** Dynamic vertical effects for a 150-foot span bridge.

## 8 CONCLUSIONS AND RECOMMENDATIONS

Bridge dynamic analysis provides a basis to study the impact of high-speed train loads on structures, particularly at resonant speeds. These speeds will produce the maximum vertical effect for normal bridge rating calculations. It isn't necessarily the application of the speed assigned to the territory that produces the greatest vertical effect but rather the train speed that coincides with the natural vibration period of the structure.

The dynamic vertical effects are highly sensitive to the bridge's natural frequency, wheel spacing, train speed, and bridge length. Determination of beam deflection amplitudes associated with resonant speeds for different bridge lengths is of particular interest. With any type of beam vibration there is a corresponding velocity and acceleration associated with the motion of the structure.

By evidence of comparison with field results, a mathematical model can be created to represent a bridge girder's response to a moving train. Field results used to verify the model can be summarized as follows:

1. Working Train Deflections and Strains—6 mph
2. Working Train Deflections and Strains—41 mph
3. Acela Train Deflections and Strains—120 mph
4. Acela Train Deflections and Strains—145 mph
5. Byers Report Impact Values—60 mph to 80 mph, 70 mph to 90 mph, and 80 mph to 100 mph.

From the mathematical model, realistic bridge ratings can be determined for varying span lengths and train speeds greater than 90 mph. Fittingly, it is recommended that a dynamic analysis be performed for train speeds of greater than 120 mph (within reasonable bridge natural frequency limits) and included in the AREMA MRE as an amendment to bridge rating guidelines. If a structure is not within reasonable natural frequency limits, the train speed threshold of 120 mph for a dynamic analysis may not be appropriate. The guidelines can be introduced by the AREMA High Speed Rail Ad Hoc Committee in the form of a ballot for a vote and implemented by the industry if approved. Acceptance of the ideas for a dynamic analysis can be achieved through the AREMA approval process with support from Amtrak and, perhaps, members of the Transportation Research Board's Rail Safety IDEA Committee.

## 9 FUTURE RESEARCH AND CRITERIA DEVELOPMENT

Reviewing the material and documentation with respect to the subject matter also demonstrates not only the necessity to evaluate vertical effects, but the need to examine dynamic criteria. For example, bridge deck acceleration limits should be researched for ballast instability. The downward acceleration of a ballasted deck results in the loss of interlocking forces within the ballast to support the track. To control track support, it is suggested that acceleration limits be assigned to help

reduce the potential for ballast instability. In addition to bridge deck accelerations, other areas of research or criteria development may include, are but not limited to:

- Torsional vibration
- Bridge natural frequency limits
- Set of formal procedures for a complete analysis
- Suspension systems (outside scope of project).

## 10 REFERENCES

Amtrak, Locomotive and Car Diagrams (Permission granted by Amtrak for its use).

Amtrak, Engineering Practices, Bridge Load Rating Policy, Amtrak, Philadelphia Pa., 2011.

Amtrak, Plans: “N.Y. NH. & H. R. R. New London to Providence Bridge 155.85 over Usquepaug River, 1.89 Miles East of Kenyons Sta. R.I.”, Amtrak, Philadelphia, Pa., Nov. 1904.

AREMA, *Manual of Railway Engineering*, American Railway Engineering and Maintenance-of-Way Association, Lanham Md., 2009.

Biggs, J., *Introduction to Structural Dynamics*, McGraw–Hill, New York, N.Y., 1964.

Byers, W., “Impact From Railway Loading on Steel Girder Spans,” *Journal of the Structural Division, Proceedings of the American Society of Civil Engineers*, June 1970, pp. 1093–1103.

*Eurocode 1: Actions on structures—Part 2 Traffic Loads on Bridges*, British Standard BS EN 1991-2:2003, Eurocode, Brussels, Belgium, 2010.

Fryba, L., *Dynamics of Railway Bridges*, 1st ed., Thomas Telford House, London, England, 1996.

Fryba, L., *Vibration of Solids and Structures under Moving Loads*, 3rd ed., Thomas Telford House, London, England, 1999.

Kunz, F.C., *Design of Steel Bridges*, 1st ed., McGraw–Hill Book Co., New York, N.Y., 1915.

Museros, P., Romero, M.L., Poy, A., Alarcon, E., “Advances in the analysis of short span railway bridges for high-speed lines,” *Computers & Structures*, Vol. 2002, 80 pp. 2121–2132.

Paz, M. and W. Leigh, *Structural Dynamics Theory and Computation*, 5th ed., Springer Science Business Media, LLC, New York, N.Y., 2004.

Unsworth, J.F., *Design of Modern Steel Railway Bridges*, CRC Press, Boca Raton, Fla., 2010.

Waddell, J.A.L., *Bridge Engineering*, 1st ed., John Wiley & Sons, Inc., New York, N.Y., 1916.

Yang, Y.-B., *Vehicle–Bridge Interaction Dynamics: With Applications to High Speed Railways*, World Scientific Publishing Company, Inc., River Edge, N.J., 2004.

Yang, Y.-Bin, J.-D. Yau, and L.-C. Hsu, “Vibration of simple beams due to trains moving at high speeds,” *Engineering Structures*, Vol. 19, No. 11, 1977, pp. 936–944.

Zacher, M., “Dynamic of Railroad Bridges,” presentation at the 5th ADAMS/Rail User Conference, Haarlem, the Netherlands, 2000.